Rydberg Atom-Enabled Spectroscopy of Polar Molecules via Förster Resonance Energy Transfer

Sabrina Patsch,[†] Martin Zeppenfeld,[‡] and Christiane P. Koch[*,†]

[†]*Dahlem Center for Complex Quantum Systems and Fachbereich Physik, Freie Universität Berlin, Arnimallee 14, 14195 Berlin, Germany*
[‡]*Max-Planck-Institut für Quantenoptik, Hans-Kopfermann-Straße 1, 85748 Garching, Germany*

E-mail: christiane.koch@fu-berlin.de

Abstract

Non-radiative energy transfer between a Rydberg atom and a polar molecule can be controlled by a DC electric field. Here we show how to exploit this control for state-resolved, non-destructive detection and spectroscopy of the molecules where the lineshape reflects the type of molecular transition. Using the example of ammonia, we identify the conditions for collision-mediated spectroscopy in terms of the required electric field strengths, relative velocities, and molecular densities. Rydberg atom-enabled spectroscopy is feasible with current experimental technology, providing a versatile detection method as basic building block for applications of polar molecules in quantum technologies and chemical reaction studies.

TOC Graphic

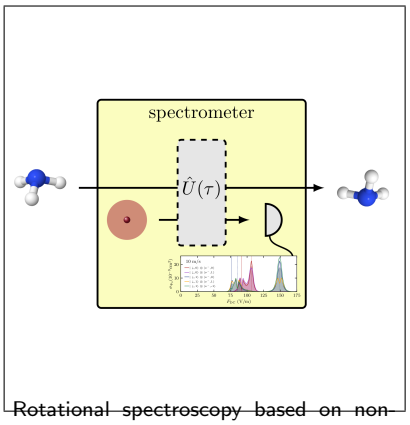

Rotational spectroscopy based on non-radiative energy transfer with a Rydberg atom rather than light-matter interaction is suggested.

Cold polar molecules are excellent candidates for quantum control with applications ranging from fundamental physics[1,2] and quantum information[3–5] to cold chemistry.[6] The ability to detect the molecules, ideally at the single molecule level and in a non-destructive and state-resolved fashion, is a prerequisite to any such application. Optical detection schemes such as laser-induced fluorescence or absorption[7–10] are destructive and difficult to apply at low density except for select molecules with optical cycling transitions. An alternative approach to non-destructive detection suggested the use of Rydberg atoms.[11,12] It exploits, instead of driving molecular transitions by laser light, Förster resonant energy transfer (FRET), i.e., non-radiative energy exchange between donor and acceptor mediated by resonant dipole-dipole interaction.[13,14] Rydberg atoms are particularly well suited to FRET due to their large dipole moment.[15,16] Rydberg states are readily prepared,[17,18] and the scaling of Rydberg transitions with the principal quantum number[19] allows for covering the microwave and terahertz spectral range, i.e., rotational transition frequencies in a large variety of molecules.[12] Basic feasibility of non-destructive detection of molecules via FRET with Rydberg atoms has been demonstrated for ammonia,[20] as has electric field control of the energy transfer.[20–22] The latter leverages the easy tunability of Rydberg energy levels, due to their sensitiv-

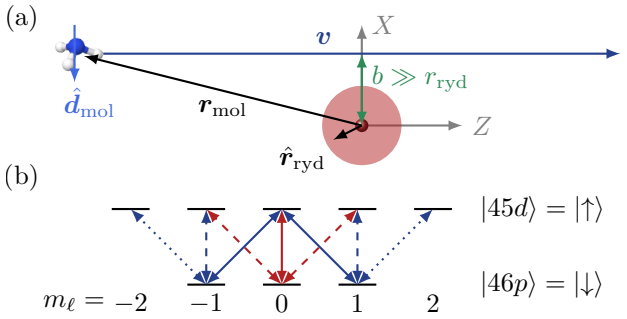

Figure 1: Collision-mediated Rydberg spectroscopy of polar molecules relies on the interaction of the molecular dipole moment (light-blue arrow) with the electric field due to the charge distribution of the Rydberg atom's valence electron (indicated by the shaded area). (a) Classical scattering trajectory (dark blue). (b) Relevant energy levels of the Rydberg atom with all possible dipole transitions indicated by arrows.

ity to external fields.[23,24] Thanks to this tunability it should be possible to use FRET not only to see whether a molecule is present or not but to actually infer the molecular state prior to the interaction. This would be an extremely useful tool for quantum technologies and studies of cold and ultracold chemistry but requires a description of the molecular structure beyond the popular two-level approximation.[4,5,12,20–22,25–27]

Here, we establish a first principles-based theoretical framework for FRET in collisions of polar molecules with Rydberg atoms and predict electric field-dependent cross sections with full account of the interparticle dynamics. In an experiment, the cross sections will be obtained by measuring the final state of the Rydberg atom via, e.g., ionization as a function of the electric field. Whether the cross sections display well-resolved lines suitable for spectroscopy depends on the key parameter governing a collision, the relative velocity. Well-resolved lines, in turn, allow for inferring the state of the molecule or molecular ensemble, as we show below. Such Rydberg spectroscopy of polar molecules only requires existence of (near) resonant dipole transitions in the two particles.

Translational motion of the collision complex and internal degrees of freedom can be separated due to their different time and energy scales,[28] similarly to the semi-classical impact parameter method.[29] The distance $\boldsymbol{r}_{\rm mol}(t)$ between molecule and atomic core, cf. Fig. 1(a), is then a time-dependent parameter in the atom-molecule interaction. The Hamiltonian for the internal degrees of freedom is given by

$$\hat{H}(t) = \hat{H}_{\rm ryd} + \hat{V}_{\rm ryd}^{\rm DC} + \hat{H}_{\rm mol} + \hat{V}_{\rm int}(t)\,, \qquad (1)$$

where $\hat{V}_{\rm ryd}^{\rm DC}$ captures the Stark shifts in the Rydberg atom due to the DC electric field.[30] $\hat{V}_{\rm int}(t)$ describes the interaction of the molecular electric dipole moment $\hat{\boldsymbol{d}}_{\rm mol}$ with the electric field arising from the charge distribution of the Rydberg atom's valence electron. For sufficiently large distances between atom and molecule, it is given by the dipole-dipole contribution,

$$\hat{V}_{\rm dd}(t) = \frac{e}{4\pi\varepsilon_0}\left(\frac{\hat{\boldsymbol{d}}_{\rm mol}\cdot\hat{\boldsymbol{r}}_{\rm ryd}}{r_{\rm mol}^3(t)} - \frac{3\big(\hat{\boldsymbol{d}}_{\rm mol}\cdot\boldsymbol{r}_{\rm mol}(t)\big)\big(\hat{\boldsymbol{r}}_{\rm ryd}\cdot\boldsymbol{r}_{\rm mol}(t)\big)}{r_{\rm mol}^5(t)}\right), \qquad (2)$$

where $\hat{\boldsymbol{r}}_{\rm ryd}$ is the position of the Rydberg electron. We assume the ensemble to be sufficiently dilute such that a Rydberg atom interacts at most once with a molecule[28] and neglect any change of the molecular trajectory due to the interaction,

$$\boldsymbol{r}_{\rm mol}(t) = vt\,\boldsymbol{e}_Z + b\,\boldsymbol{e}_X \qquad (3)$$

with $v\boldsymbol{e}_Z$ the velocity, b the impact parameter, and the molecular beam direction chosen parallel to the DC field. We expect the best resolved spectra for this geometry due to symmetry; different orientations of the trajectory imply a dependence on the azimuthal angle and thus an additional averaging. The Rydberg atom is assumed to change its state only due to FRET with the molecule. We denote the probability for this state change by $P_{\rm ex}^{\Psi_0}(\Delta, b)$ for a given initial state $|\Psi_0\rangle$ of atom and molecule with Δ the energy mismatch between the molecular and atomic transition. To calculate $P_{\rm ex}^{\Psi_0}(\Delta, b)$, we solve the time-dependent Schrödinger equation with $\hat{H}(t)$, chosing initial and final time

such that atom and molecule are well separated and $\hat{V}_{\rm dd}(t)$ is negligible. The corresponding cross section is obtained by integrating this probability over all impact parameters,

$$\sigma_{\Psi_0}(\Delta) = 2\pi \int_0^\infty b\, db\, P_{\rm ex}^{\Psi_0}(\Delta, b)\,. \qquad (4)$$

Electric field tunability of the cross section arises from tuning Δ via the Stark effect of the Rydberg atom. The semiclassical approximation holds down to a velocity of about $v = 0.1\,\mathrm{m/s}$.[28] This is also the lower limit for spectroscopy since, for even smaller velocities, the Rydberg atom will likely decay before the particles had enough time to interact.[28]

Motivated by recent experiments,[20,22] we consider FRET between Rydberg atoms and the inversion mode of ammonia. The molecular state can be written in terms of the vibrational inversion mode $|\nu^\pm\rangle$ and the symmetric top eigenstates $|JKM\rangle$.[28] Since rotational transition frequencies are large compared to the inversion splitting, it is sufficient to consider a single inversion doublet at a time, such that $|\nu^\pm JKM\rangle$ with $|\nu^+\rangle$ the lowest, symmetric and $|\nu^-\rangle$ the second lowest, anti-symmetric sub-level of the inversion doublet for given J, K and M. Coupling to other vibrational or electronic degrees of freedom is negligible. The inversion splitting depends on J and K approximately as[31]

$$\omega_{\rm inv} = \omega_{\rm inv}^0 - c_1\left(J(J+1) - K^2 + c_2K^2\right)\,. \quad (5)$$

with constants $c_{1,2}$.[31] For fixed J and K, dipole transitions obey the selection rules $\nu^\pm \leftrightarrow \nu^\mp$ and $\Delta M = \pm 1$ or $\Delta M = 0$ (unless $M = 0 = M'$).

$\hat{H}_{\rm ryd}$ is represented in the spherical basis $|n\ell, m_\ell\rangle$ with principal quantum number n, angular quantum number ℓ and projection m_ℓ. Assuming rubidium, levels with $\ell \leq 7$ are shifted, due to the finite size of the ionic core,[32] by the quantum defect $\delta_{n\ell j}$ which we approximate as $\delta_{n\ell} \approx \delta_{n\ell,j=\ell+\frac{1}{2}}$.[28] For low J and $K = J$, the inversion splitting of ammonia is matched by transitions between $|46p, m_\ell\rangle \equiv |\downarrow, m_\ell\rangle$ and $|45d, m'_\ell\rangle \equiv |\uparrow, m'_\ell\rangle$, cf. Fig. 1(b). For $J = K = 1$, the energy mismatch between the atomic and molecular transitions is shown in Fig. 2(a) as a function of the DC field strength. It vanishes at different field strengths for transitions involving different m_ℓ. This is at the core of the suggested spectroscopy.

We consider two different scenarios, both of which can be realized with existing experimental setups. In the first one, we assume the molecule to be prepared in a single rotational energy level, for example in an experiment with a suitable (e.g. quadrupole) guide or Stark decelerator.[33–35] In the second scenario, we consider molecules in essentially arbitrary rotational states taking a thermal state as example and show that this state can be inferred from the measurements. The two scenarios differ in the number of state-to-state cross sections that have to be averaged when predicting the outcome of an experiment. Both rely on FRET between atom and molecule and both assume state-resolved detection of the Rydberg atom after the collision.

Starting with the first scenario of molecules in a single rotational level, we assume $J = K = 1$ for the molecule and the Rydberg atom in one of the states $|\downarrow, m_\ell\rangle$ with $m_\ell = 0, \pm 1$. The choice of m_ℓ is easily ensured by a suitable laser polarization in the Rydberg state preparation. Since the energy transfer is resonant, it is sufficient to consider only the upper inversion level for the molecule, $|\nu^-, M\rangle$ with $M = 0, \pm 1$. The state-to-state cross sections for all possible initial states are shown as a function of the DC field strength for three relative velocities in Fig. 2(b-d) with resonances indicated by vertical lines. As the velocity increases, the cross section peaks increase in width and decrease in amplitude. For dipole-dipole transitions, the maximum of the cross section and its line width scale as[12]

$$\max(\sigma) \propto d_{\rm mol}/v, \quad \Delta \propto v^{3/2}/\sqrt{d_{\rm mol}} \qquad (6)$$

with $d_{\rm mol} \propto K/\sqrt{J(J+1)}$ for the considered transition in symmetric top molecules.[36]

Molecules in a molecular beam experiment are randomly oriented, corresponding to all M states being populated. We thus consider two M-averaged cross sections, for $m_\ell = 0$ and $m_\ell = 1$ (shaded areas in Fig. 2(b-

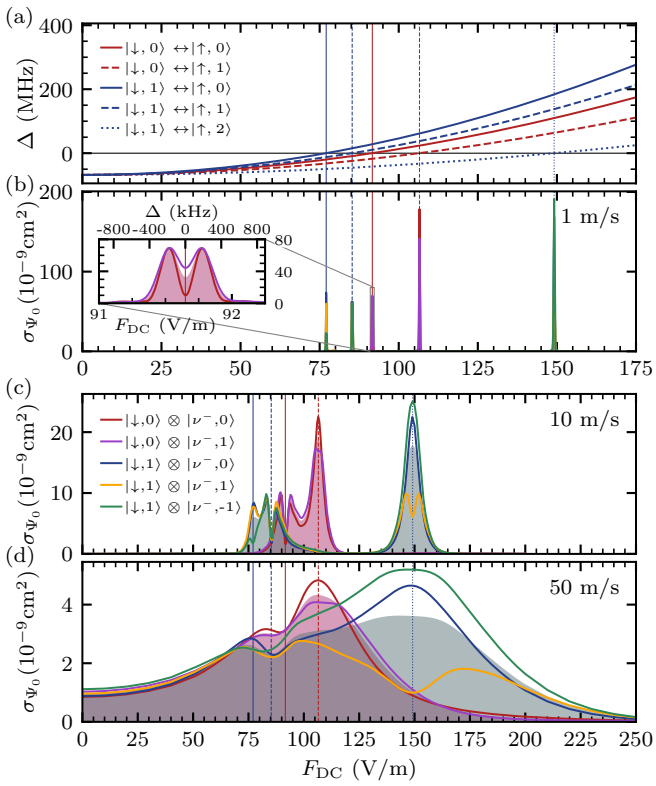

Figure 2: Electric field control of collisions between molecules prepared in a single rotational energy level (here $J = 1 = K$) and Rydberg atoms: (a) Energy mismatch Δ between the inversion mode of ammonia and the Rydberg transitions shown in Fig. 1(b). Vertical lines indicate resonances. (b-d) State-to-state cross sections for different initial states (indicated by line color) and velocities (panels). Red (green) shaded areas show cross sections averaged over degenerate initial molecular states with the atom in $|\downarrow, 0\rangle$ ($|\downarrow, 1\rangle$). Note the different scales of the x- and y-axes.

d)): At low velocities, the peaks do not overlap (Fig. 2(b)) and are clearly distinguishable also for higher velocities (Fig. 2(c)). While the resolution of single transitions is hampered at increasing velocity, the two M-averaged cross sections continue to be distinguishable up until about $v = 50\,\mathrm{m/s}$ (Fig. 2(c)). In particular, the two resonances occurring at the largest field strengths, corresponding to $|\downarrow, m_\ell = 0; \nu^-, M\rangle \leftrightarrow |\uparrow, m_\ell = 1; \nu^+, M'\rangle$ for the dashed red and $|\downarrow, m_\ell = 1; \nu^-, M\rangle \leftrightarrow |\uparrow, m_\ell = 2; \nu^+, M'\rangle$ for the dotted blue vertical lines, can be resolved. It is thus possible to deduce from the recorded cross sections the molecular energy splitting and hence the rotational level. At higher velocities, this is no longer the case.

The peak heights in Fig. 2(b-d) imply that an effective volume of $2 \cdot 10^{-9}\,\mathrm{cm}^3$ is probed by one Rydberg atom, assuming an interaction time of $100\,\mu\mathrm{s}$. This suggests a fully saturated signal at a molecular density of $5 \cdot 10^8\,\mathrm{cm}^{-3}$. In experiments, the molecular signal has to be discriminated against the background, mainly due to Rydberg transitions caused by blackbody radiation.[20] Given the cross sections in Fig. 2(b-d), this should be possible for densities as low as $10^5\,\mathrm{cm}^{-3}$.[28]

Various lineshapes are observed in Fig. 2(b-c), even in the M-averaged case. For example, if the Rydberg atom starts in $m_\ell = 0$ (vertical red lines), the cross section around 107 V/m (dashed) is Lorentzian but displays a clear dip around 92 V/m (solid, see inset). We now show that it is the time-dependence of the interaction (2) due to the collision that is reflected in the lineshape.

The selection rules allow for three types of FRET transitions, cf. Fig. 3(a), which we term criss-cross (red), and linear (blue) and diagonal (green) flip-flop. In order to analyze each type separately, we reduce the Hilbert space of atom and molecule to only two states each, the ones connected by the respective transitions in Fig. 3(a). Then there is only a single matrix element for the interaction, $V_{\rm dd}(t) = \langle\downarrow, m_\ell; \nu^-, M|\hat{V}_{\rm dd}(t)|\uparrow, m'_\ell; \nu^+, M'\rangle$, shown in Fig. 3(b) for $v = 100\,\mathrm{m/s}$ and $b = 160\,\mathrm{nm}$. It is symmetric as a function of time

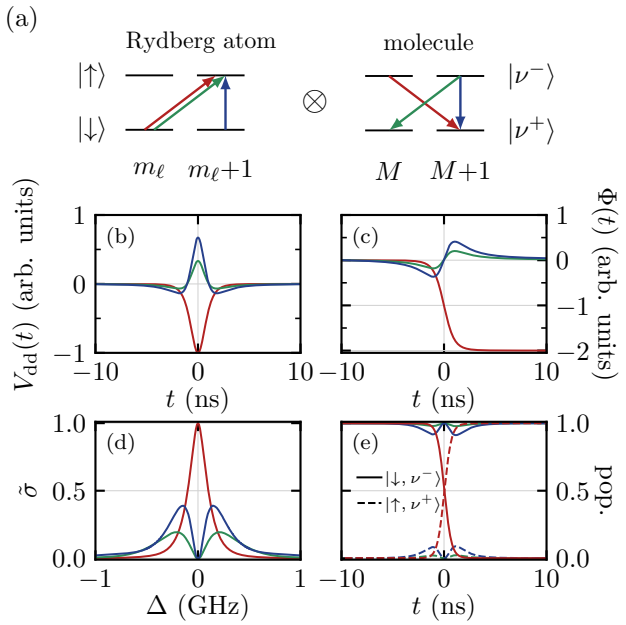

Figure 3: Types of transitions in two two-level systems due to dipole-dipole coupling (a) and their behaviour during the collision (b-e). (b) interaction strength $\hat{V}_{\rm dd}(t)$ scaled to a maximal absolute value of 1, (c) its integrated value $\Phi(t)$; (e) exemplary time evolution at resonance; (d) normalized cross-section $\tilde{\sigma} = \sigma/\sigma_{\rm max}$ as a function of the energy mismatch Δ (with $\sigma_{\rm max} = 1.7 \cdot 10^{-9}\,{\rm cm}^2$).

around $t = 0$ where the two particles are closest to each other and $V_{\rm dd}(t)$ takes its extremal value. The two coupled two-level systems (TLS) accumulate a relative phase, which in the resonant case is simply given by $\Phi(t) = \int_{-\infty}^{t} V_{\rm dd}(t')dt'$, shown in Fig. 3(c). For the criss-cross transitions (red lines), $V_{\rm dd}(t)$ is always negative, $\Phi(t)$ thus decreases monotonically, the two TLS exchange their excitation perfectly (Fig. 3(e)), and the TLS cross section displays a Lorentzian peak (Fig. 3(d)). For flip-flop transitions (green and blue lines in Fig. 3(b-e)), the non-Lorentzian lineshapes are rationalized by the different time evolution of $V_{\rm dd}(t)$ with two changes of sign. Phase accumulation is then non-monotonic and, most importantly, the phase equals zero at $t = 0$. This causes the TLS to return to their initial states, cf. Fig. 3(e), resulting in a vanishing cross section at resonance. Shifting the transitions away from resonance breaks the symmetry in the time evolution of $V_{\rm dd}(t)$, resulting in non-vanishing accumulated phase and cross section. This behavior is observed for both linear and diagonal flip-flop transitions since only the overall strength of their coupling differs.

While the cross sections in Fig. 2 arise from more complex dynamics than that of two coupled TLS, the peaks resemble lineshapes as seen in Fig. 3(d). For example, the peak at 107 V/m for the initial state $|\downarrow, m_\ell = 0\rangle \otimes |\nu^-, M = 1\rangle$ (purple line) is Lorentzian, suggesting a criss-cross transition where both m_ℓ and M change by one. Indeed, we numerically find the transition to $|\uparrow, m_\ell = -1\rangle \otimes |\nu^+, M = 0\rangle$ to be dominant. In contrast, around 92 V/m, the peak shows a deep dip due to a flip-flop transition to $|\uparrow, m_\ell = 0\rangle \otimes |\nu^+, M = 1\rangle$. Note that the state-to-state cross-sections in Fig. 2 do not vanish entirely at resonance because our model includes all m_ℓ/M-sub-levels. Repeating the analysis for all initial states in Fig. 2, we find all resonances to be dominated by one type of transition.[28] The electric field controlled cross sections thus reveal whether a criss-cross or a flip-flop transition is at the core of a resonance.

We now discuss the second scenario, showing how to employ Rydberg spectroscopy to infer the population of molecular states. Figure 4 illustrates the working principle, correlating rotational states with peaks in the cross section. The dependence of the M-averaged cross section on the rotational quantum numbers J and K, shown in Fig. 4(a), can be observed as a function of the DC field strength, due to dependence of the inversion splitting on J and K, cf. Eq. (5). Figure 4 focusses on states with the Rydberg atom initially in $m_\ell = 0$ (for $m_\ell = 1$ cf. Ref. 28) and molecules in $J \leq 11$ which have an inversion splitting near-resonant to the Rydberg transition at the considered electric field strengths and temperatures. The cross sections in Fig. 4(a) display a sequence of resonances, similarly to Fig. 2(b), with the position and height of the peaks depending on K, in perfect agreement with the scaling of Eq. (6). When considering a thermal ensemble, the cross sections are obtained by averaging over all states in the ensemble, cf. Fig. 4(b,c). The occupation of the rotational states is then given by

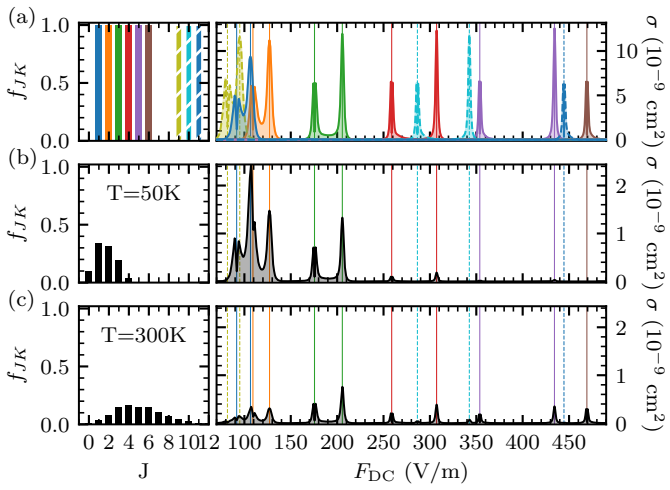

Figure 4: Rydberg spectroscopy with M-averaged cross sections shown on the right (for $v = 10\,\mathrm{m/s}$ and $m_\ell = 0$) and relative populations of the rotational states shown on the left for single rotational levels (a) and thermal ensembles (b,c) at rotational temperatures of 50 and 300 K, respectively. The vertical lines indicate resonances, solid lines correspond to $K = J$, dashed lines to $K = J-1$ (other molecular transitions are far off-resonant).

$f_{JK}(T) = g/\mathcal{N} e^{-\frac{E_{JK}}{k_B T}}$ with T the temperature, $\mathcal{N}$ a normalisation factor, and g the statistical weight of the state.[28] At very low temperatures, $T \leq 10\,\mathrm{K}$, the $J = K = 1$ contribution dominates, leading to a similar pattern as shown in Fig. 2(b). At higher rotational temperatures (Fig. 4(b,c)), an increasing number of rotational states contributes. For a relative velocity of $v = 10\,\mathrm{m/s}$, as shown in Fig. 4, the resonances are easily resolved and assigned to the different rotational states. The resonances for $J = 1, 2$ between 70 and 140 V/m are the hardest to resolve but Fig. 2 shows that this is possible until at least 50 m/s. Provided the velocity is sufficiently low, measurement of the cross section as a function of the electric field strength thus allows for inferring the rotational state composition of the molecular ensemble from the position and height of the peaks. An explicit example is worked out in Ref. 28. In order to determine the composition of states with other K values, simply a different Rydberg transition has to be selected, e.g. $|47p, m_\ell\rangle$ to $|46d, m'_\ell\rangle$.

In summary, we have derived the principles of a collision-mediated, non-destructive spectroscopy of polar molecules, using a complete dynamical description from first principles. Instead of light-matter interaction, the spectroscopy is based on resonant dipole-dipole interaction with Rydberg atoms. Taking ammonia and rubidium as example, we have shown that electric field control of the cross sections allows for inferring the relative population of rotational states for velocities below 100 m/s. The lineshape reveals the dominant type of FRET-induced transition. For very low velocities, of the order of 1 m/s, linewidths below 1 MHz will be obtained. The considered velocities between 100 m/s and 1 m/s cover the range relevant for application of the suggested spectroscopy in cold reaction dynamics and quantum technologies. A key advantage of Rydberg atom-enabled spectroscopy is the ability to measure spectra for extremely low molecular density. Detection of single molecules in optical tweezers or at molecular densities as low as $10^5\,\mathrm{cm}^{-3}$ seems realistic.

Our example of ammonia and rubidium is easily carried over to other atomic and molecular species. Exchanging rubidium by helium,[22] for instance, mainly reduces the quantum defects, rendering the isolation of a suitable dipole-dipole transition from neighbouring (possibly higher-order) transitions somewhat more difficult. When replacing ammonia by other polar molecules, purely rotational transitions can be used instead of the inversion mode.[12] A further prospect is to probe transitions governed by higher order terms in the multipole expansion; this simply requires a suitable choice of Rydberg levels. A method for state-resolved non-destructive detection of polar molecules addresses an essential need for their application in quantum technologies and cold reaction dynamics studies and establishes Rydberg atoms as a versatile addition to the quantum control toolbox for cold and ultracold molecules.[4,5,25–27]

Acknowledgement We thank Ed Narevicius, Ronnie Kosloff, and Melanie Schnell for insightful discussions. Financial support from the Studienstiftung des deutschen Volkes e.V. and the Deutsche Forschungsgemeinschaft via

the Priority Programme GiRyd (KO 2301/14-1 Grant No. 428456483) and Grant No. ZE 1096/2-1 is gratefully acknowledged.

References

(1) Hutzler, N. R. Polyatomic molecules as quantum sensors for fundamental physics. *Quantum Science and Technology* **2020**, *5*, 044011.

(2) Mitra, D.; Leung, K. H.; Zelevinsky, T. Quantum control of molecules for fundamental physics. *Phys. Rev. A* **2022**, *105*, 040101.

(3) Albert, V. V.; Covey, J. P.; Preskill, J. Robust Encoding of a Qubit in a Molecule. *Physical Review X* **2020**, *10*, 031050.

(4) Wang, K.; Williams, C. P.; Picard, L. R. B.; Yao, N. Y.; Ni, K.-K. Enriching the quantum toolbox of ultracold molecules with Rydberg atoms. *arXiv:2204.05293* **2022**,

(5) Zhang, C.; Tarbutt, M. R. Quantum computation in a hybrid array of molecules and Rydberg atoms. *arXiv:2204.04276* **2022**,

(6) Dulieu, O., Osterwalder, A., Eds. *Cold Chemistry*; Theoretical and Computational Chemistry Series; The Royal Society of Chemistry, 2018.

(7) Shuman, E. S.; Barry, J. F.; Glenn, D. R.; DeMille, D. Radiative force from optical cycling on a diatomic molecule. *Physical Review Letters* **2009**, *103*, 223001.

(8) Wang, D.; Neyenhuis, B.; de Miranda, M. H.; Ni, K. K.; Ospelkaus, S.; Jin, D. S.; Ye, J. Direct absorption imaging of ultracold polar molecules. *Physical Review A* **2010**, *81*, 061404(R).

(9) Cheuk, L. W.; Anderegg, L.; Augenbraun, B. L.; Bao, Y.; Burchesky, S.; Ketterle, W.; Doyle, J. M. Λ-Enhanced Imaging of Molecules in an Optical Trap. *Phys. Rev. Lett.* **2018**, *121*, 083201.

(10) Shaw, J. C.; Schnaubelt, J. C.; McCarron, D. J. Resonance Raman optical cycling for high-fidelity fluorescence detection of molecules. *Phys. Rev. Research* **2021**, *3*, L042041.

(11) Kuznetsova, E.; Rittenhouse, S. T.; Sadeghpour, H. R.; Yelin, S. F. Rydberg-atom-mediated nondestructive readout of collective rotational states in polar-molecule arrays. *Phys. Rev. A* **2016**, *94*, 032325.

(12) Zeppenfeld, M. Nondestructive detection of polar molecules via Rydberg atoms. *EPL (Europhysics Letters)* **2017**, *118*, 13002.

(13) Förster, T. Zwischenmolekulare Energiewanderung und Fluoreszenz. *Annalen der Physik* **1948**, *437*, 55–75.

(14) Andrews, D. L.; Demidov, A. A. *Resonance Energy Transfer*; Wiley, 1999.

(15) Safinya, K. A.; Delpech, J. F.; Gounand, F.; Sandner, W.; Gallagher, T. F. Resonant Rydberg-Atom-Rydberg-Atom Collisions. *Physical Review Letters* **1981**, *47*, 405–408.

(16) Ravets, S.; Labuhn, H.; Barredo, D.; Béguin, L.; Lahaye, T.; Browaeys, A. Coherent dipole–dipole coupling between two single Rydberg atoms at an electrically-tuned Förster resonance. *Nature Physics* **2014**, *10*, 914–917.

(17) Haroche, S.; Raimond, J.-M. *Exploring the Quantum. Atoms, Cavities, and Photons*; Oxford University Press: New York, 2006.

(18) Larrouy, A.; Patsch, S.; Richaud, R.; Raimond, J.-M.; Brune, M.; Koch, C. P.; Gleyzes, S. Fast Navigation in a Large Hilbert Space Using Quantum Optimal Control. *Physical Review X* **2020**, *10*, 021058.

(19) Šibalić, N.; Adams, C. S. *Rydberg Physics*; IOP Publishing, 2018; pp 1–27.

(20) Jarisch, F.; Zeppenfeld, M. State resolved investigation of Förster resonant energy transfer in collisions between polar molecules and Rydberg atoms. *New Journal of Physics* **2018**, *20*, 113044.

(21) Zhelyazkova, V.; Hogan, S. D. Electrically tuned Förster resonances in collisions of NH_3 with Rydberg He atoms. *Phys. Rev. A* **2017**, *95*, 042710.

(22) Gawlas, K.; Hogan, S. D. Rydberg-State-Resolved Resonant Energy Transfer in Cold Electric-Field-Controlled Intrabeam Collisions of NH3 with Rydberg He Atoms. *Journal of Physical Chemistry Letters* **2020**, *11*, 83–87.

(23) Facon, A.; Dietsche, E.-K.; Grosso, D.; Haroche, S.; Raimond, J.-M.; Brune, M.; Gleyzes, S. A sensitive electrometer based on a Rydberg atom in a Schrödinger-cat state. *Nature* **2016**, *535*, 262–265.

(24) Adams, C. S.; Pritchard, J. D.; Shaffer, J. P. Rydberg atom quantum technologies. *Journal of Physics B* **2020**, *53*, 012002.

(25) Kuznetsova, E.; Rittenhouse, S. T.; Beterov, I. I.; Scully, M. O.; Yelin, S. F.; Sadeghpour, H. R. Effective spin-spin interactions in bilayers of Rydberg atoms and polar molecules. *Phys. Rev. A* **2018**, *98*, 043609.

(26) Huber, S. D.; Büchler, H. P. Dipole-Interaction-Mediated Laser Cooling of Polar Molecules to Ultracold Temperatures. *Phys. Rev. Lett.* **2012**, *108*, 193006.

(27) Zhao, B.; Glaetzle, A. W.; Pupillo, G.; Zoller, P. Atomic Rydberg Reservoirs for Polar Molecules. *Phys. Rev. Lett.* **2012**, *108*, 193007.

(28) See supplemental material [url] for technical details, which includes Refs.[37–40].

(29) Beigman, I.; Lebedev, V. Collision theory of Rydberg atoms with neutral and charged particles. *Physics Reports* **1995**, *250*, 95–328.

(30) The Stark effect of the molecule is negligible at the relevant field strengths.[31]

(31) Townes, C. H.; Schawlow, A. L. *Microwave Spectroscopy*; Dover Publications, Inc.: New York, 1975.

(32) Gallagher, T. F. *Rydberg atoms*; Cambridge Monographs on Atomic, Molecular, and Chemical Physics; Cambridge University Press: Cambridge, 1994.

(33) Petitjean, L.; Gounand, F.; Fournier, P. R. Collisions of rubidium Rydberg-state atoms with ammonia. *Physical Review A* **1986**, *33*, 143.

(34) Bethlem, H. L.; Crompvoets, F. M. H.; Jongma, R. T.; van de Meerakker, S. Y. T.; Meijer, G. Deceleration and trapping of ammonia using time-varying electric fields. *Physical Review A* **2002**, *65*, 053416.

(35) Chervenkov, S.; Wu, X.; Bayerl, J.; Rohlfes, A.; Gantner, T.; Zeppenfeld, M.; Rempe, G. Continuous centrifuge decelerator for polar molecules. *Physical Review Letters* **2014**, *112*, 013001.

(36) Kroto, H. W. *Molecular Rotation Spectra*; John Wiley and Sons Ltd.: New York, 1975.

(37) Šibalić, N.; Pritchard, J. D.; Adams, C. S.; Weatherill, K. J. ARC: An open-source library for calculating properties of alkali Rydberg atoms. *Computer Physics Communications* **2017**, *220*, 319–331.

(38) Meschede, D. Centimeter-wave spectroscopy of highly excited rubidium atoms. *Journal of the Optical Society of America B* **1987**, *4*, 413–419.

(39) Han, J.; Jamil, Y.; Norum, D. V. L.; Tanner, P. J.; Gallagher, T. F. Rb nf quantum defects from millimeter-wave spectroscopy of cold ^{85}Rb Rydberg atoms. *Physical Review A* **2006**, *74*, 054502.

(40) Nussenzveig, P. Mesures de champs au niveau du photon par interférométrie atomique. Ph.D. thesis, Université Pierre et Marie Curie - Paris VI, France, 1994.